Catalysis Today xxx (2016) xxx–xxx

Contents lists available at ScienceDirect

Catalysis Today

journal homepage: www.elsevier.com/locate/cattod

# Activity and selectivity of different base catalysts in synthesis of guaifenesin from guaiacol and glycidol of biomass origin

Shivaji L. Bhanawase, Ganapati D. Yadav*

*Department of Chemical Engineering, Institute of Chemical Technology, Nathalal Parekh Marg, Matunga, Mumbai 400 019, India*

ARTICLE INFO

*Article history:*
Received 20 July 2016
Received in revised form 27 October 2016
Accepted 1 December 2016
Available online xxx

*Keywords:*
Guaifenesin (or (RS)-3-(2-methoxyphenoxy) propane-1,2-diol)
Guaiacol (or 2-methoxyphenol) and glycidol (or 2,3-epoxy-1-propanol)
Biomass valorization
Hydrotalcite
Calcined hydrotalcite
Green chemistry
Kinetics

ABSTRACT

Guaiacol and glycidol can be obtained from biomass valorization. Guaiacol (2-methoxyphenol) and glycidol (2,3-epoxy-1-propanol) have been used for the efficient synthesis of guaifenesin ((RS)-3-(2-methoxyphenoxy) propane-1,2-diol). Different catalysts such as hydrotalcite (HT), calcined hydrotalcite (CHT), calcinated hydrotalcite supported on hexagonal mesoporous silica, magnesium oxide, alumina and, potassium promoted zirconium oxide were synthesized, out of which CHT was found to be the most active, selective and reusable catalyst. The catalyst characterization was done by different techniques. Both Oxide and hydroxide phases were observed on calcination of HT in air at 450 °C for 6 h. CHT possess both acidic and basic sites and basicity of CHT was the highest. Crystallite size, surface area and pore size of CHT play important role in catalytic activity and selectivity. Reaction was carried out in a batch reactor and influence of different parameters was systematically studied. The reaction mechanism involving two sites, acidic and basic, was proposed. A suitable kinetic model was developed and fitted against experimental data. A second order rate equation was derived on the basis of Langmuir–Hinshelwood–Hougen–Watson mechanism with weak adsorption of reactants, intermediates and products. Kinetics was used to predict reaction conditions to obtain guaifenesin selectively. Guaifenesin was efficiently obtained with 94.8% selectivity at guaiacol conversion of 38.2% over CHT at 80 °C after 4 h.



## 1. Introduction

In the foreseeable future, the stocks of fossil fuels would have been exhausted and it would be necessary to derive chemicals and fuels from renewable resources [1–3]. A variety of fresh and waste biomass ought to be subjected to chemical, biological and extractive technologies to derive platform chemicals, fuels and materials [4]. Lignin is abundantly available as a waste from the paper and pulp industries. In this regard, lignin will be an important source for conversion into a spectrum of intermediates which could be further valorized [5]. Similarly, glycerol, a co-product of biodiesel production, can be catalytically transformed into a number of bulk chemicals such as acrolein, acrylic acid, 1,2-propanediol, 1,3-propanediol, etc. [6–8]. Guaiacol (2-methoxyphenol) and glycidol (2,3-epoxy-1-propanol) have been obtained from biomass from lignin and glycerol, respectively [9,10].

Synthesis of guaifenesin from renewable sources should result in a greener and more sustainable process. One of the possible paths to produce guaifenesin is based on biomass-derived guaiacol and glycidol by using heterogeneous catalysis which has been at the hub of green chemistry leading to waste reduction, process intensification and profitability. Hydrotalcites (for instance, $Mg_6Al_2(OH)_{16}CO_3{\cdot}4H_2O$) have been used as solid base catalysts for various reactions [11–17] and can be used for the production of guaifenesin. Hydrotalcite is a bifunctional catalyst having both base (major) and acid (minor) sites. It has a layered double hydroxide structure in which positively charged magnesium-aluminum layers are formed due to defects in the structure. Defects are formed by replacement of magnesium by aluminum. Anions such as carbonate, nitrate, hydroxide and chloride are present at the interlayer. On calcination at 500–800 °C, mixed magnesium-aluminum oxides are formed with large surface area with basic and acidic sites. Acid and basic properties can be adjusted with change in metal and metal composition [18,19].

Guaifenesin is an expectorant drug used in racemic form for the treatment of cough, asthma, gout, fibromyalgia, to facilitate conception and to improve voice [20]. Generally, guaifenesin is synthesized by Williamson's etherification reaction in which nucleophile of guaiacol attacks on glycidol, epichlorohydrin, 1-chloroglycerol, glycerol carbonate, 3-bromo-1-propene and isopropylidene glycerol [21–26]. Homogeneous bases such as triethyl

* Corresponding author.
*E-mail addresses:* gdyadav@yahoo.com, gd.yadav@ictmumbai.edu.in (G.D. Yadav).

http://dx.doi.org/10.1016/j.cattod.2016.12.008
0920-5861/

amine, sodium hydroxide, potassium carbonate are used in stoichiometric quantities and neutralized at the end of reaction causing environmental pollution problems. The literature review suggests that guaifenesin synthesis has not been so far reported using heterogeneous catalysis. In this work, we report a novel protocol for the synthesis of guaifenesin using guaiacol and glycidol catalyzed by calcined hydrotalcite (CHT). The reaction is additive and 100% atom economical. Influences of different parameters are studied including reaction mechanism and kinetics.

## 2. Experimental

Following catalysts were prepared and further characterized by various techniques, details of which are included in supporting information.

### 2.1. Preparation of catalysts

#### 2.1.1. Hydrotalcite (HT)

The synthesis process is different and modified from that reported in literature [27]. HT of Mg: Al ratio 3:1 was prepared by co-precipitation method. Solution of magnesium nitrate (7.66 g, 0.03 mol) and aluminium nitrate (3.79 g, 0.01 mol) in 30 mL distilled water was prepared. Solution of sodium hydroxide (3.6 g, 0.09 mol) and sodium carbonate (2.8 g, 0.027 mol) in 30 mL distilled water was prepared. At constant pH (9), both the solutions were added simultaneously to a round bottom flask (500 mL) with overhead stirrer at a speed of 300 rpm immersed in oil bath at temperature 30 °C. White precipitate of HT was obtained and further digested at 60 °C for 12 h. HT obtained was washed with distilled water to get neutral pH to the supernatant solution. HT was filtered and then dried at 100 °C for 24 h to obtain dry lumps. HT lumps were crushed in mortar to get fine powder of weight 2.8 g. HT powder was calcined at 450 °C for 6 h to get calcined HT (CHT) [27].

#### 2.1.2. Hexagonal mesoporous silica supported hydrotalcite (HMSSH)

Hexagonal mesoporous silica (HMS) was prepared by a known procedure [28]. HMSSH (10% w/w) of Mg: Al ratio 3:1 was prepared by co-precipitation method. In a conical flask, solution of magnesium nitrate (2.29 g, 0.009 mol) and aluminium nitrate (1.14 g, 0.003 mol) in 50 mL distilled water was prepared. In another conical flask, solution of sodium hydroxide (1.08 g, 0.027 mol) and sodium carbonate (0.85 g, 0.008 mol) in 50 mL distilled water was prepared. Five g of HMS was added to a round bottom flask (250 mL) with overhead stirrer at a speed of 300 rpm immersed in oil bath at temperature 30 °C. At constant pH (9), both the solutions were added simultaneously to the round bottom flask, white precipitate of HT was obtained, which further was digested at 60 °C for 12 h. Material so obtained was washed with distilled water to get neutral pH to the supernatant solution. Then material was filtered and dried at 100 °C for 12 h to obtain dry powder. It was crushed in mortar to get fine powder which was calcined at 450 °C for 6 h [11,29].

#### 2.1.3. Potassium modified zirconium hydroxide (PMZH)

PMZH (8.8% w/w) was prepared by wet impregnation method. Zirconium hydroxide was synthesized by a known procedure [30,31]. 0.25 g of potassium nitrate was dissolved in 1.5 mL of distilled water. This solution was added to 1 g of zirconium hydroxide under stirring to get wet material which was dried in oven at 100 °C for 12 h. It was crushed in mortar to get fine powder which was calcined at 600 °C for 3 h [32].

#### 2.1.4. Aluminium oxide

Aluminium hydroxide was synthesized by co-precipitation method from aluminium nitrate by following the same procedure described in preparation of hydrotalcite (Section 2.1.1). Aluminium hydroxide was calcined at 450 °C in a furnace for 6 h to get aluminium oxide ($Al_2O_3$).

#### 2.1.5. Magnesium oxide

Magnesium hydroxide was synthesized by co-precipitation method from magnesium nitrate. The same procedure described in preparation of hydrotalcite (Section 2.1.1) was followed. Magnesium hydroxide was calcined at 450 °C in a furnace for 6 h to get magnesium oxide (MgO).

**Table 1**
TPD analysis of catalysts, PMZH, MgO, CHT, HMSSH, and $Al_2O_3$.

| Catalyst | PMZH | MgO | CHT | HMSSH | $Al_2O_3$ |
|---|---|---|---|---|---|
| Acidity (mmol $g^{-1}$) | 0.09 | 0.41 | 0.68 | 0.63 | 0.76 |
| Basicity (mmol $g^{-1}$) | 0.49 | 0.75 | 1.53 | 0.48 | 0.32 |

### 2.2. Reaction procedure

In a typical reaction, autoclave reactor (details included in supporting information) was charged with guaiacol (0.0081 mol), glycidol (0.020 mol), tetrahydrofuran (THF) (10 mL) and 0.03 g $mL^{-1}$ (0.9 g) of the catalyst. The total organic phase volume was made to 30 mL with THF. An initial sample was taken at the desired temperature. The reaction mixture was stirred with mechanical stirrer at the desired speed, and samples were collected periodically. For control reaction, speed of agitation was 1000 rpm and temperature was 120 °C at self-generated pressure. Reaction samples were analyzed by HPLC (details included in supporting information). Synthesis of guaifenesin (3-(2-methoxyphenoxy)propane-1,2-diol) and byproduct (2-(2-methoxyphenoxy)propane-1,3-diol) from condensation reaction of guaiacol and glycidol is shown in Scheme 1.

## 3. Results and discussions

### 3.1. Catalyst characterization

TPD (temperature programmed desorption) analysis of the catalysts PMZH, MgO, CHT, HMSSH, and $Al_2O_3$ was carried out to find out the strength of acidic and basic sites (Table 1). Acidity (except $Al_2O_3$) and basicity of CHT was the highest. In the case of CHT, $NH_3$ desorption peak was observed at 123 °C corresponding to weak as well as strong acidic sites of concentration 0.68 mmol $g^{-1}$ (Fig. S1). Two $CO_2$ desorption peaks were observed, first peak at 116 °C corresponding to weak basic sites of concentration 0.95 mmol $g^{-1}$ and second peak at 264 °C corresponding to strong basic sites of concentration 0.58 mmol $g^{-1}$ (Fig. S2) [12,17,33].

All the catalysts were analyzed for surface area analysis. All showed, type IV adsorption–desorption isotherm with hysteresis loop of type H1, which is a characteristic of a mesoporous solid (Fig. 1). The Brunauer–Emmett–Teller (BET) surface area, Langmuir surface area, pore size, and pore volume of all the catalysts are shown in Table 2. Surface area of PMZH was the lowest. Surface area of HMSSH was the highest while pore size was the lowest. After calcination, surface area of hydrotalcite increases due to formation of mixed Mg-Al metal oxides. On calcination, due to evolution of $CO_2$ and $H_2O$, more porous material is formed by the formation of pores through the layers. Hydrotalcites containing carbonates and showing such behavior have been reported [27]. BET surface area of CHT was measured to be 240.5 $m^2$ $g^{-1}$. The pore volume and pore diameter were 0.97 mL $g^{-1}$ and 159.2 Å, respectively. Pore width of CHT was in range of 100–600 Å (Fig. S3).

The XRD (X-ray diffraction) pattern of HT have sharp reflections at 11.2°, 22.5°, 34.2°, 38.2°, 45.0°, 60.0°, and 61.3° (JCPDS 22-700) corresponding to (003), (006), (012), (015), (018), (110),

Please cite this article in press as: S.L. Bhanawase, G.D. Yadav, Activity and selectivity of different base catalysts in synthesis of guaifenesin from guaiacol and glycidol of biomass origin, Catal. Today (2016), http://dx.doi.org/10.1016/j.cattod.2016.12.008

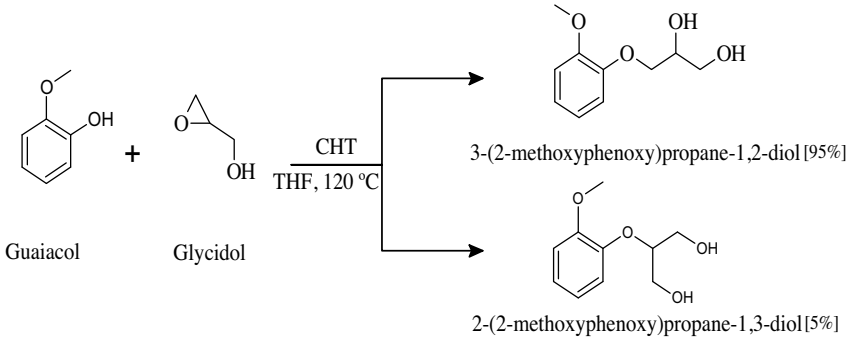


**Scheme 1.** Condensation of guaiacol and glycidol.

**Table 2**
Surface area analysis of catalysts, PMZH, MgO, CHT, HMSSH, $Al_2O_3$, and HT.

| Catalyst | BET Surface Area ($m^2\ g^{-1}$) | Langmuir Surface Area ($m^2\ g^{-1}$) | Pore Volume ($cm^3\ g^{-1}$) | Pore Size (Å) |
|---|---|---|---|---|
| PMZH | 16.7 | 24.2 | 0.12 | 290.7 |
| HT | 76.7 | 113.5 | 0.84 | 388 |
| MgO | 140.5 | 207.7 | 0.36 | 84.1 |
| CHT | 240.5 | 352.4 | 0.97 | 159.2 |
| $Al_2O_3$ | 273.1 | 401.3 | 0.51 | 70.4 |
| HMSSH | 344.4 | 504.2 | 0.45 | 56.9 |

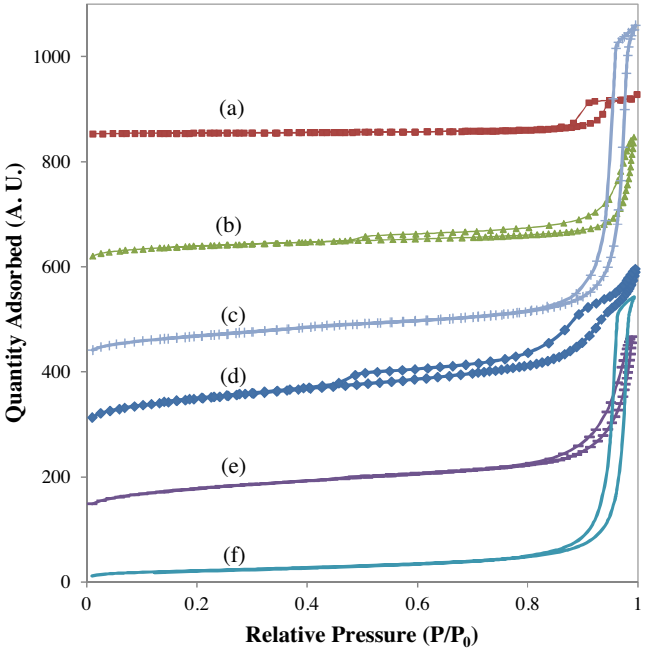


**Fig. 1.** $N_2$ adsorption-desorption isotherm of catalysts (a) PMZH, (b) MgO, (c) CHT, (d) HMSSH, (e) $Al_2O_3$, and (f) HT.

(113) planes, respectively (Fig. 2). HT after calcination in air at 450 °C for 6 h gives amorphous structure (CHT), showing reflections at 11.4°, 23.0°, 34.2°, 38.2°, 43.3° and 62.6° (JCPDS 87-0653) corresponding to (003), (006), (012), (015), (200) and (220) planes, respectively (Fig. 2). The layered double hydroxide was converted to mixed oxide manifested by the presence of new broad reflections at 43.31°, 62.58° which correspond to the (200) and (220) planes. CHT has almost all the reflections shown by HT but the intensity of peaks is low and some new peaks of mixed oxides structure have appeared. Due to incomplete oxidation, both hydroxide and oxide phases were obtained. In general, calcination of HT in nitrogen at 450 °C gives pure mixed metal oxide phase. Hydrotalcite shows memory effect which is well reported in literature [12]. In presence of water, mixed Mg-Al metal oxides is again converted to corresponding hydroxides. This is the reason for the incomplete oxidation of HT, even after calcination in air at 450 °C. Crystallite size of the HT and CHT was 25.8 and 7.7 nm, respectively, which also proves that amorphous nature of CHT.

FTIR analysis of HT and CHT is shown in Fig. S4. HT have characteristic bands of water at 1650 $cm^{-1}$, interaction of $H_2O$—$CO_3^{2-}$ around 3000 $cm^{-1}$, hydroxyls in the 3400–3600 $cm^{-1}$ region and carbonates at 1517 $cm^{-1}$. In the case of CHT, the bands below 1000 $cm^{-1}$ are the vibration modes for Mg—O and Al—O in the mixed oxide [16]. In CHT, peaks of water at 1650 $cm^{-1}$, interaction of $H_2O$—$CO_3^{2-}$ around 3000 $cm^{-1}$, hydroxyls in the 3400–3600 $cm^{-1}$ region and carbonates at 1517 $cm^{-1}$ disappear or peaks intensity decreases which indicates formation of mixed metal oxide.

TGA of the HT and CHT is shown in Fig. S5. HT loses 34% of a total weight; the first weight loss at temperatures below 200 °C was attributed to the loss of physically adsorbed and interlayer water molecules, whereas the second weight loss (200–450 °C) originates from the conversion of metal hydroxide to metal oxide and decomposition of carbonates in the interlayer. CHT loses 23% of the total weight which may be due to the presence of both oxide and hydroxide phases, the moisture content, and the adsorbed $CO_2$ in the sample.

Figs. S6 and S7 show SEM images of HT and CHT, respectively. Both show irregular particle shape and the average particle size is in the range of 50–100 μm. EDXS analysis confirmed the presence of Mg and Al elements. In the case of HT, the observed Mg and Al mol ratio was 2.9:1 and for CHT, the observed Mg and Al mol ratio was 3.1:1 which was in agreement with expected mol ratio, 3:1 (Table S1). TEM images of HT and CHT are shown in Figs. S8 and S9, respectively. HT particles are of spherical shape while particles of CHT are irregular spherical shape and relatively porous in nature.

### 3.2. Efficacy of various catalysts

Activity of different catalysts such as HMSSH, PMZH, MgO, $Al_2O_3$, HT, and CHT was evaluated for conversion and selectivity

Please cite this article in press as: S.L. Bhanawase, G.D. Yadav, Activity and selectivity of different base catalysts in synthesis of guaifenesin from guaiacol and glycidol of biomass origin, Catal. Today (2016), http://dx.doi.org/10.1016/j.cattod.2016.12.008

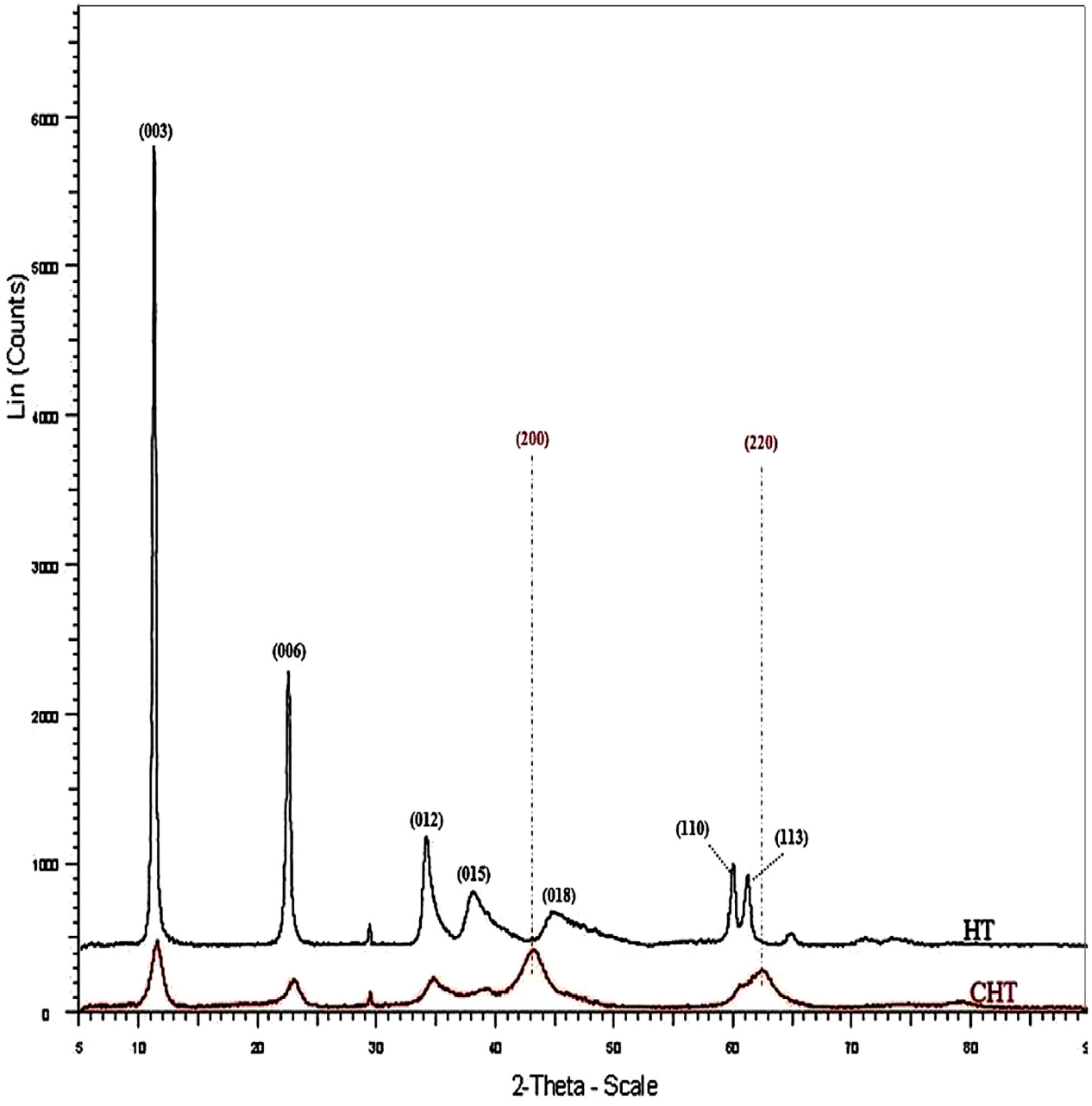


**Fig. 2.** X-ray diffraction (XRD) of catalysts HT and CHT.

of the reaction (Fig. 3). In the absence of catalyst (Nil) only negligible conversion (0.7%) was observed. Order of catalysts conversion was as follows: PMZH (99%) > HT (70.3%) > CHT (66.5%) > MgO (42.5%) > HMSSH (5%) > $Al_2O_3$ (1.3%). While order of catalysts selectivity was as follows: $Al_2O_3$ (100%) > CHT (93.5%) > MgO (92%) > HT (87.6%) > PMZH (81.8%) > HMSSH (59%). PMZH appeared to be the best for conversion but its selectivity for product was the lowest which was due to lowest surface area and larger pore size with respect to CHT (Table 2). HT and CHT gave almost the same conversion, but selectivity of CHT for the product was greater than HT which might be due to crystallite size, surface area and pore size. Crystallite size of the CHT was lower (7.7 nm) than HT (25.8 nm). Surface area of CHT (240.5 $m^2\ g^{-1}$) was higher than HT (76.7 $m^2\ g^{-1}$). Pore size of CHT (159.2 Å) is lower than HT (388 Å). Lower pore size of CHT was contributing for its superior selectivity. High activity of CHT was due to its highest basicity and acidity (except $Al_2O_3$) in comparison to other catalysts (Table 1). CHT was found to be best for the reaction considering selectivity and activity of catalyst towards the product. Hence CHT was used in further experiments.

### 3.3. Effect of speed of agitation

Fig. 4 depicts the effect of speed of agitation on conversion from 800 to 1200 rpm to observe that the conversion profile. At 1000 and 1200 rpm, conversion was almost the same thereby indicating the absence of external mass transfer resistance for transport of reactants to the external surface of the catalyst particle from the bulk liquid phase. A theoretical calculation was also done as delineated in some of our earlier work to confirm that there was no influence of external mass transfer resistance [31,34]. Thus, further experiments were carried out at 1000 rpm.

Please cite this article in press as: S.L. Bhanawase, G.D. Yadav, Activity and selectivity of different base catalysts in synthesis of guaifenesin from guaiacol and glycidol of biomass origin, Catal. Today (2016), http://dx.doi.org/10.1016/j.cattod.2016.12.008

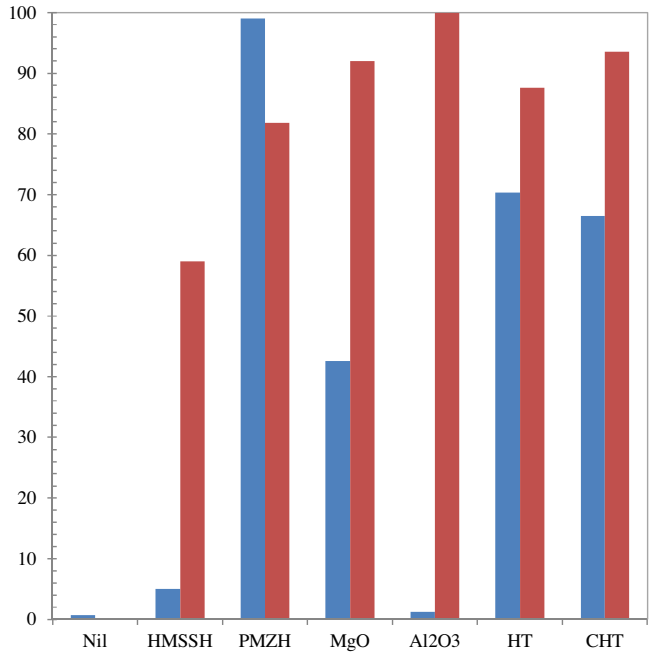


**Fig. 3.** Efficacy of various catalysts: guaiacol; 0.0081 mol, glycidol; 0.02 mol, speed of agitation; 1000 rpm, catalyst loading; 0.03 g mL$^{-1}$, temperature; 120 °C, solvent; THF, total volume; 30 mL, duration; 4 h, autogenous pressure, % conversion (■), % selectivity (■).

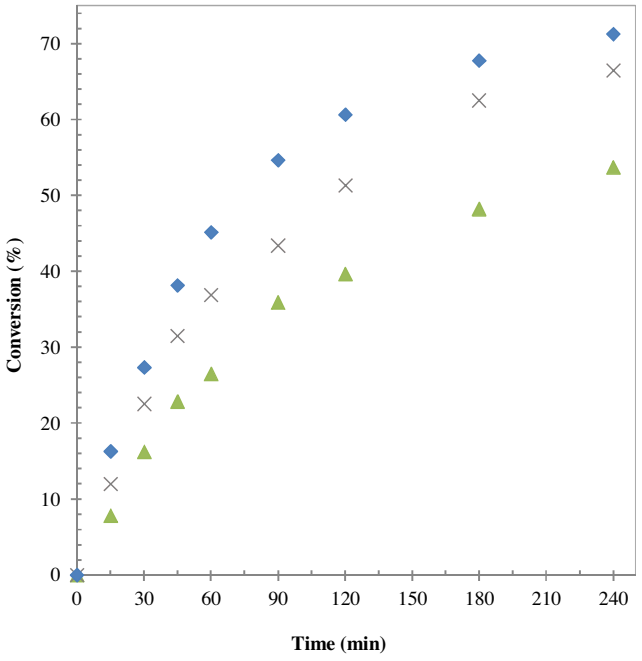


**Fig. 5.** Effect of catalyst loading: catalyst; CHT, guaiacol; 0.0081 mol, glycidol; 0.02 mol, speed of agitation; 1000 rpm, temperature; 120 °C, solvent; THF, total volume; 30 mL, duration; 4 h, autogenous pressure, 0.02 g mL$^{-1}$ (▲), 0.03 g mL$^{-1}$ (✕), 0.04 g mL$^{-1}$ (◆).

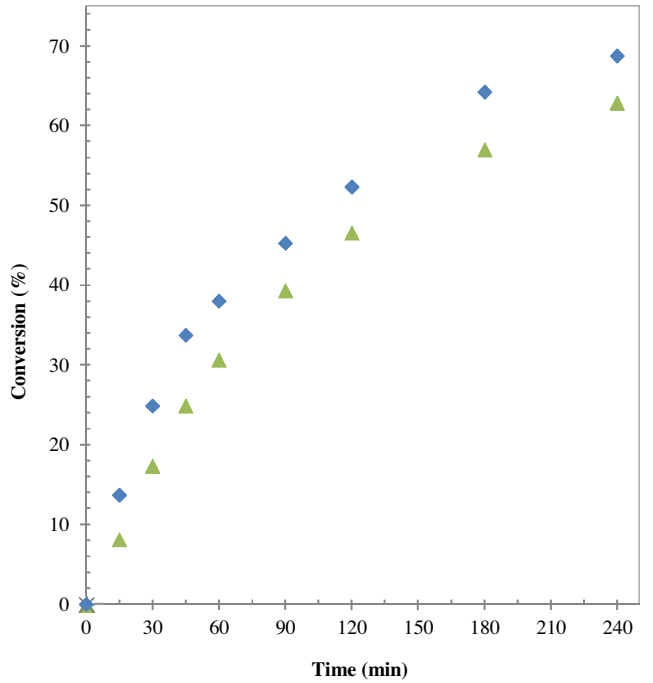


**Fig. 4.** Effect of speed of agitation: catalyst; CHT, guaiacol; 0.0081 mol, glycidol; 0.02 mol, catalyst loading; 0.03 g mL$^{-1}$, temperature; 120 °C, solvent; THF, total volume; 30 mL, duration;4 h, autogenous pressure, 800 rpm (▲), 1000 rpm (✕), 1200 rpm (◆).

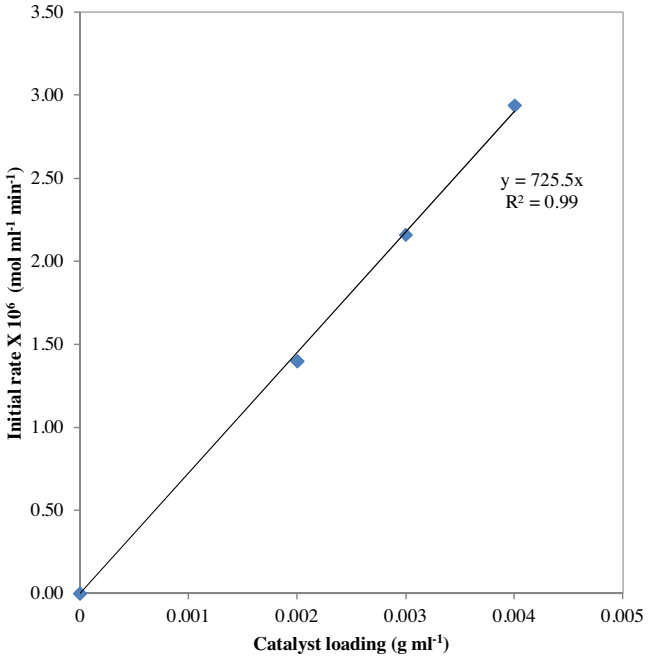


**Fig. 6.** Plot of initial rate versus catalyst loading: catalyst; CHT, guaiacol; 0.0081 mol, glycidol; 0.02 mol, speed of agitation; 1000 rpm, temperature; 120 °C, solvent; THF, total volume; 30 mL, autogenous pressure.

### 3.4. Effect of catalyst loading

After confirmation of absence of external mass transfer resistance, the effect of catalyst loading on initial rate of reaction and overall conversion was studied from 0.02 to 0.04 g mL$^{-1}$ of total volume of reaction mass (Fig. 5). A plot of initial rate against catalyst loading showed that initial rate of reaction was directly proportional to the catalyst loading (Fig. 6) which was due to the proportional increase in active sites thereby confirming the absence of external mass transfer and intra-particle diffusion resistances. In order to ascertain that the intra-particle diffusion resistance was totally absent, the Wiesz-Prater modulus was calculated using observed rates of reaction, as discussed earlier, which showed values far less than one [31,34].

Please cite this article in press as: S.L. Bhanawase, G.D. Yadav, Activity and selectivity of different base catalysts in synthesis of guaifenesin from guaiacol and glycidol of biomass origin, Catal. Today (2016), http://dx.doi.org/10.1016/j.cattod.2016.12.008

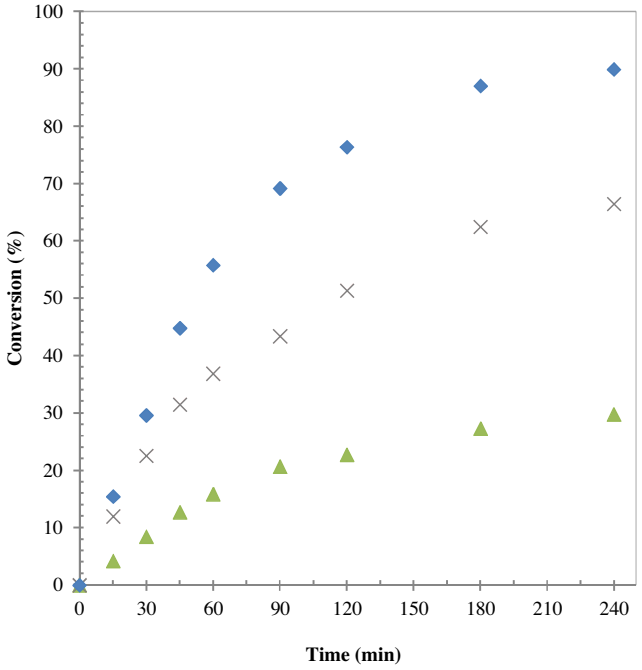


**Fig. 7.** Effect of mole ratio: catalyst; CHT, guaiacol; 0.0081 mol, speed of agitation; 1000 rpm, catalyst loading, 0.03 g $mL^{-1}$, temperature; 120 °C, solvent; THF, total volume; 30 mL, duration; 4 h, autogenous pressure, 1:1 (▲), 1:2.5 (×), 1:5 (◆).

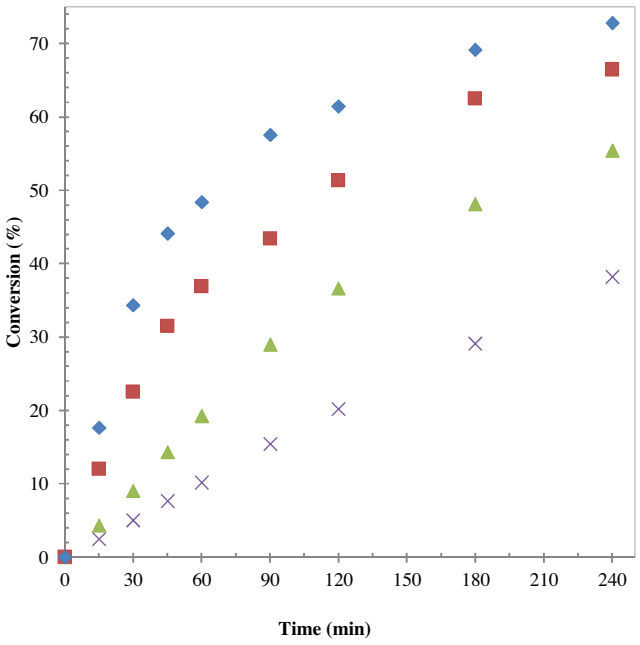


**Fig. 8.** Effect of temperature: catalyst; CHT, guaiacol; 0.0081 mol, glycidol; 0.02 mol, speed of agitation; 1000 rpm, catalyst loading; 0.03 g $mL^{-1}$, solvent; THF, total volume; 30 mL, duration; 4 h, autogenous pressure, 80 °C (×), 100 °C (▲), 120 °C (■), 140 °C (◆).

### 3.5. Effect of mole ratio

In the absence of external mass transfer and intra-particle diffusion resistances, overall rate of reaction would be controlled by other resistances, namely, adsorption, surface reaction and desorption. Adsorption of the reacting species will be key factor for the rate of reaction. To verify this fact, the effect of mole ratio was studied. Mole ratio of guaiacol to glycidol was varied from 1:1 to 1:5 by keeping the total volume the same. With increase in concentration of glycidol, conversion was found to increase. As concentration of glycidol with respect to guaiacol increases, greater will be the adsorption of glycidol on the catalyst sites which will increase the concentration of electrophile to react with guaiacol resulting in higher conversion of guaiacol. At 1:5 mol ratio the highest conversion was obtained (Fig. 7), while at 1:1 mol ratio the least conversion was obtained which was due to the concentration effect of typical power law rate.

### 3.6. Effect of temperature

This is a parallel reaction. Selectivity of products may change with increase in temperature. Effect of temperature on the selectivity and rate of reaction was studied at 80, 100, 120, and 140 °C (Fig. 8). With increase in temperature, conversion was found to increase and selectivity of guaifenesin was found to decrease. From an Arrhenius plot, calculated energy of activation for formation of guaiacol was 16.8 kcal $mol^{-1}$. The rates and conversions were strongly dependent on temperature, suggest kinetically controlled regime.

### 3.7. Reusability of catalyst

Reusability studies were conducted for three experiments. After completion of the reaction and lowering the temperature, the reaction mass was filtered to separate the catalyst. The catalyst was refluxed with 30 mL THF for 1 h to remove any adsorbed reaction ingredients. Then the catalyst was separated by filtration followed by drying at 100 °C for 12 h to get an off-white material which was calcined at 450 °C for 6 h to get whitish material. In all processes, catalyst loss during filtration and handling was compensated by addition of corresponding fresh catalyst for next three experiments. There was no significant decrease in conversion of guaiacol and selectivity of product (Fig. 9).

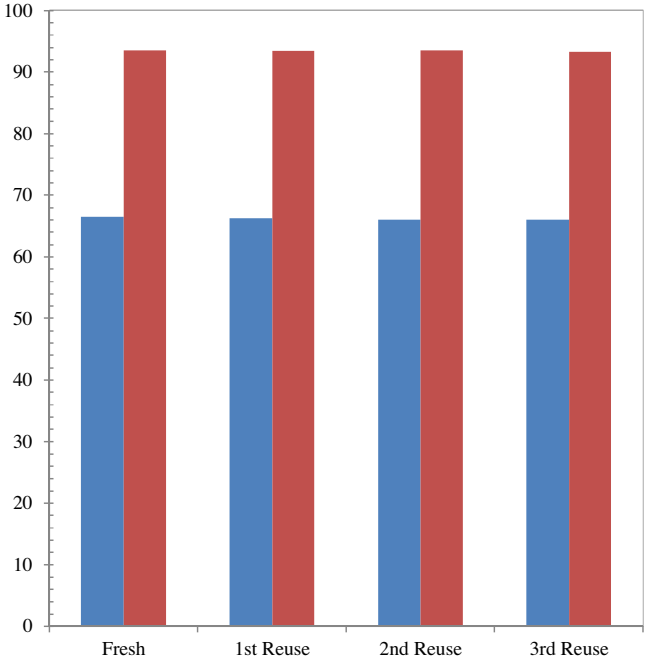


**Fig. 9.** Catalyst reusability: catalyst; CHT, guaiacol, 0.0081 mol, glycidol; 0.02 mol, speed of agitation; 1000 rpm, catalyst loading; 0.03 g $mL^{-1}$, temperature; 120 °C, solvent; THF, total volume; 30 mL, duration; 4 h, autogenous pressure, % conversion (■), % selectivity (■).

Regenerated catalyst was characterized different techniques to verify the properties in comparison with fresh catalyst. Surface area

Please cite this article in press as: S.L. Bhanawase, G.D. Yadav, Activity and selectivity of different base catalysts in synthesis of guaifenesin from guaiacol and glycidol of biomass origin, Catal. Today (2016), http://dx.doi.org/10.1016/j.cattod.2016.12.008

of regenerated catalyst was 233.9 $m^2\ g^{-1}$ while of fresh catalyst was 240.5 $m^2\ g^{-1}$ (Table S2). FTIR analysis of fresh and regenerated catalyst revealed that all functional groups were intact and showed similar bands in FTIR spectra (Fig. 6). $NH_3$ and $CO_2$ TPD analysis of fresh and regenerated catalyst showed the same acidity and basicity (Table S2). Also rate of reaction and turn over frequency for reused catalysts remain constant which confirmed that catalyst is stable and reusable (Table S3).

## 4. Reaction kinetics

### 4.1. Reaction mechanism

In CHT, $Al^{3+}$ ions replace some $Mg^{2+}$ ions which gives positively charged layered structure. It consists of both basic sites and acidic sites; basic sites are due to $O^{2-}$ anions in the layer structure and acidic sites are due to positively charged layered structure.

A possible mechanism has been proposed in Scheme 2, considering two different sites i.e. weak acid sites and basic sites. Glycidol and guaiacol get adsorbed on acidic sites and basic sites, respectively. The activation of epoxide ring at acidic sites results in formation of positive charge on the oxygen of epoxide ring. At basic sites, hydroxyl functional group of guaiacol gives $-O^{1-}$ species. The adsorbed species reacts on the surface of catalyst and results in the formation of product guaifenesin and the byproduct. Subsequently guaifenesin and byproduct get desorbed from the surface into the reaction mixture to vacate catalyst site. This catalyst site can further get involved for next catalytic cycle.

### 4.2. Kinetic model

The catalyst CHT is bifunctional with sites $S_1$ (basic) and $S_2$ (acidic) uniformly distributed on the pore surface. According to the Langmuir–Hinshelwood–Hougen–Watson (LHHW) mechanism, guaiacol (A) and glycidol (B) were assumed to adsorb on $S_1$ and $S_2$, respectively.

#### 4.2.1. Adsorption

Adsorption of guaiacol (A) on a vacant site $S_1$ is given by:

$$A + S_1 \overset{K_A}{\leftrightarrow} AS_1 \tag{1}$$

Adsorption of glycidol (B) on a vacant site $S_2$ is given by:

$$B + S_2 \overset{K_B}{\leftrightarrow} BS_2 \tag{2}$$

#### 4.2.2. Surface reaction

Surface reaction of $AS_1$ and $BS_2$ leads to the formation of $DS_2$ (chemisorbed guaifenesin) and $ES_2$ (chemisorbed 2-(2-methoxyphenoxy) propane-1, 3-diol) by two parallel reactions given by:

$$AS_1 + BS_2 \overset{k_1}{\leftrightarrow} DS_2 + S_1 \tag{3}$$

$$AS_1 + BS_2 \overset{k_2}{\leftrightarrow} ES_2 + S_1 \tag{4}$$

#### 4.2.3. Desorption

Desorption of guaifenesin ($DS_2$) and 2-(2- methoxyphenoxy) propane-1, 3-diol ($ES_2$) is given by:

$$DS_2 \overset{1/K_D}{\leftrightarrow} D + S_2 \tag{5}$$

$$ES_2 \overset{1/K_E}{\leftrightarrow} E + S_2 \tag{6}$$

The total concentration of the basic and acidic sites, $C_T$ expressed as:

$$C_{T_1} = C_{S_1} + C_{AS_1} \tag{7}$$

$$C_{T_2} = C_{S_2} + C_{BS_2} + C_{ES_2} + C_{DS_2} \tag{8}$$

The concentrations of adsorbed species are given by the following equations:

$$C_{AS_1} = K_A C_A C_{S_1} \tag{9}$$

$$C_{BS_2} = K_B C_B C_{S_2} \tag{10}$$

$$C_{ES_2} = K_E C_E C_{S_2} \tag{11}$$

$$C_{DS_2} = K_D C_D C_{S_2} \tag{12}$$

Now Eq. (7) can be written as:

$$C_{T_2} = C_{S_1} + K_A C_A C_{S_1} \tag{13}$$

Or

$$C_{S_1} = \frac{C_{T_1}}{(1+K_A C_A)} \tag{14}$$

And Eq. (8) can be written as:

$$C_{T_2} = C_{S_2} + K_B C_B C_{S_2} + K_D C_D C_{S_2} + K_E C_E C_{S_2} \tag{15}$$

Or

$$C_{S_2} = \frac{C_{T_2}}{(1+K_B C_B + K_D C_D + K_E C_E)} \tag{16}$$

The rate of formation of product D, assuming reaction to be irreversible, is given by:

$$\frac{dC_D}{dt} = k_1 K_A C_A C_{S_1} K_B C_B C_{S_2} \tag{17}$$

$$\frac{dC_D}{dt} = \frac{k_1 K_A C_A K_B C_B C_{T_1} C_{T_2}}{(1+K_A C_A)(1+K_B C_B + K_D C_D + K_E C_E)} \tag{18}$$

The value of reaction rate constant, $k_1$, can thus be evaluated by solving Eq. (18) using Polymath 6.0. We can also obtain values for equilibrium adsorption coefficients for the species A, B, D and E by solving this equation. The adsorption constants (Table 3) showed that all species were weakly adsorbed and thus an overall second order rate equation was valid.

Similarly, we can write the rate of formation of byproduct E from Eq. (4) as

$$\frac{dC_E}{dt} = \frac{k_2 K_A C_A K_B C_B C_{T_1} C_{T_2}}{(1+K_A C_A)(1+K_B C_B + K_D C_D + K_E C_E)} \tag{19}$$

The instantaneous selectivity of product D over E, $S_{D/E}$, is given by

$$S_{D/E} = \frac{dC_D/dt}{dC_E/dt} = \frac{k_1}{k_2} \tag{20}$$

Thus using Eq. (20) and selectivity ratio, the value for kinetic rate constant, $k_2$ can be evaluated (Table 3). Using the values of $k_1$ and $k_2$ obtained at different temperatures; Arrhenius plots were made for both the reactions (Fig. 10). The activation energy for the reaction guaiacol to guaifenesin ($E_1$) and guaiacol to byproduct ($E_2$) are 16.8 kcal $mol^{-1}$ and 18.3 kcal $mol^{-1}$, respectively. It indicates that the reactions are intrinsically kinetically controlled. This is an overall second order reaction.

It was observed that rate constant $k_1 > k_2$ (Table 3) and energy of activation related to these reactions; $E_1 < E_2$. The selectivity ratio ($k_1/k_2$) decrease with increase in temperature (Table 3), and activation energy for formation of byproduct is higher than activation energy for formation of guaifenesin. Thus the selectivity of guaifenesin decreases with increase in temperature due to its lower activation energy ($E_1$), while selectivity of byproduct increases with increase in temperature due to its higher activation energy ($E_2$). Hence guaifenesin synthesis is favorable at lower temperature.

Please cite this article in press as: S.L. Bhanawase, G.D. Yadav, Activity and selectivity of different base catalysts in synthesis of guaifenesin from guaiacol and glycidol of biomass origin, Catal. Today (2016), http://dx.doi.org/10.1016/j.cattod.2016.12.008

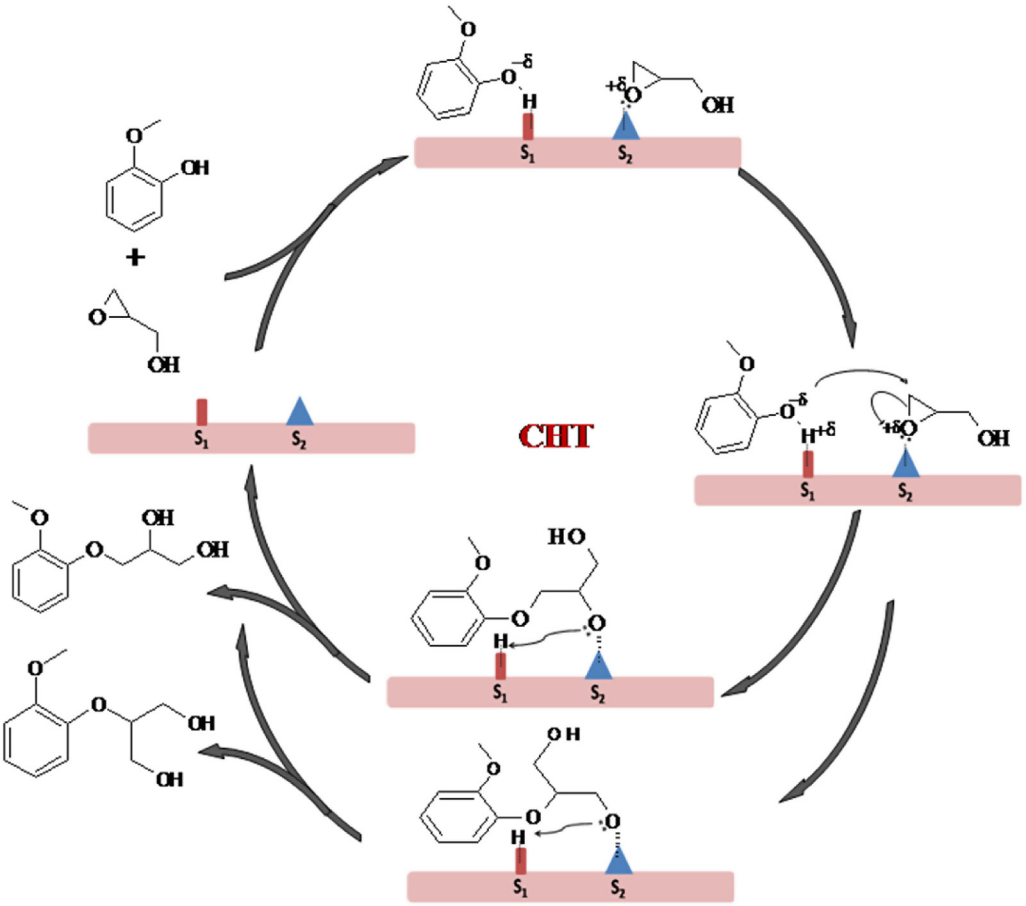


**Scheme 2.** Catalytic cycle for condensation of guaiacol and glycidol over CHT ($S_1$: base sites, $S_2$: acid sites).

**Table 3**
Reaction constant, equilibrium adsorption coefficient and selectivity ratio of reaction at different temperatures.

| Reaction temperature, °C | Equilibrium adsorption coefficient, (lit mol$^{-1}$) | | | | Reaction constant, (lit$^2$ mol$^{-1}$ s$^{-1}$ g$^{-1}$ of cat) | | Selectivity ratio, ($k_1/k_2$) |
|---|---|---|---|---|---|---|---|
| | $K_A$ | $K_B$ | $K_D$ | $K_E$ | $k_1$ | $k_2$ | |
| 80 | 0.029 | 0.013 | 0.0012 | 0.005 | $3.7 \times 10^{-3}$ | $0.2 \times 10^{-3}$ | 18.2 |
| 100 | 0.024 | 0.011 | 0.010 | 0.0046 | $9.5 \times 10^{-3}$ | $0.6 \times 10^{-3}$ | 17.4 |
| 120 | 0.019 | 0.0094 | 0.0086 | 0.0040 | $45.0 \times 10^{-3}$ | $3.1 \times 10^{-3}$ | 14.4 |
| 140 | 0.014 | 0.0080 | 0.007 | 0.0033 | $119.0 \times 10^{-3}$ | $8.5 \times 10^{-3}$ | 13.9 |

### 4.3. Validation of kinetic model

A parity plot was made to prove the fit of experimental data to the predicted according to the mathematical model (Fig. 11). Experimental rates of reaction and predicted rates of reaction show very good match which demonstrate that the assumptions made to establish kinetic model were correct.

## 5. Conclusion

Heterogeneous base catalyzed condensation of guaiacol with glycidol was studied using various catalysts. Among all catalysts, basicity and acidity (except $Al_2O_3$) of calcined hydrotalcite (CHT) was the highest. Calcination of hydrotalcite at 450 °C in air gave both hydroxide and oxide phases. CHT is a mesoporous material with high surface area. On the basis of catalyst activity and selectivity, CHT was the best and reusable catalyst due to synergistic effect of acidic and basic sites. Reaction conditions were optimized to give maximum guaiacol conversion and high selectivity for guaifenesin. Guaifenesin was obtained with 86% selectivity at guaiacol conversion of 92% over CHT at 120 °C after 4 h. Reaction kinetics was studied using LHHW model. All species were found to be weakly adsorbed and the overall reaction was second order. Activation energy for formation of guaifenesin is 16.8 kcal mol$^{-1}$. Kinetics was used to predict reaction conditions to obtain guaifenesin selectively. To obtain guaifenesin selectively, reaction may be done at following conditions: speed of agitation; 1000 rpm, temperature; 80 °C, catalyst loading; 0.03 g mL$^{-1}$, mole ratio of guaiacol to glycidol; 1:5 and solvent; THF. Guaifenesin can be efficiently obtained with 94.8% selectivity at guaiacol conversion of 38.2% over CHT at 80 °C after 4 h. Guaifenesin can be commercially synthesized by this process.

## Acknowledgements

S.L.B. thanks University Grants Commission (UGC) for awarding the Junior Research Fellowship under its Green Technology special meritorious fellowship program. G.D.Y. acknowledges support

Please cite this article in press as: S.L. Bhanawase, G.D. Yadav, Activity and selectivity of different base catalysts in synthesis of guaifenesin from guaiacol and glycidol of biomass origin, Catal. Today (2016), http://dx.doi.org/10.1016/j.cattod.2016.12.008

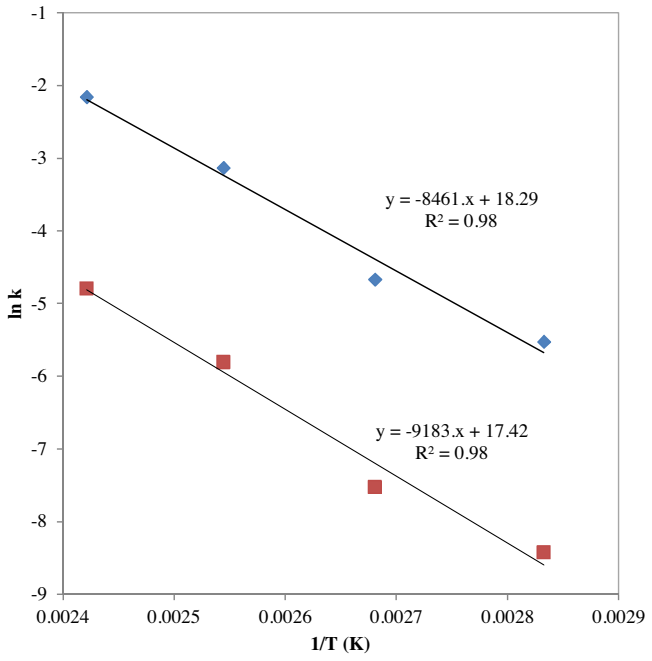


**Fig. 10.** Arrhenius plots for formation of guaifenesin and byproduct: catalyst; CHT, guaiacol; 0.0081 mol, glycidol; 0.02 mol, speed of agitation; 1000 rpm, catalyst loading; 0.03 g $mL^{-1}$, solvent; THF, total volume; 30 mL, duration; 4 h, autogenous pressure, ln $k_1$ (♦), ln $k_2$ (■).

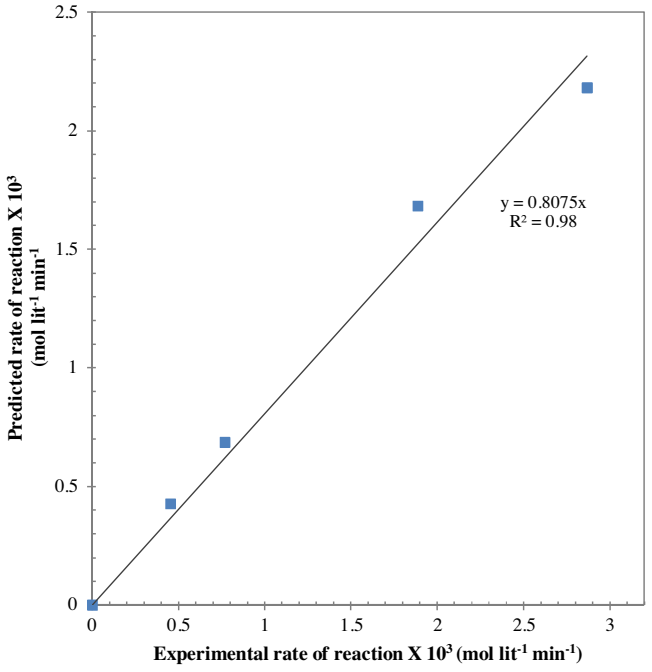


**Fig. 11.** Parity plot to demonstrate correctness of kinetic model.

from R.T. Mody Distinguished Professor Endowment of ICT and J.C. Bose National Fellowship of DST-GOI.

## Appendix A. Supplementary data

Supplementary data associated with this article can be found, in the online version, at http://dx.doi.org/10.1016/j.cattod.2016.12.008.

## References

[1] J. Zakzeski, P.C. Bruijnincx, A.L. Jongerius, B.M. Weckhuysen, The catalytic valorization of lignin for the production of renewable chemicals, Chem. Rev. 110 (2010) 3552–3599.
[2] X. Tong, Y. Ma, Y. Li, Biomass into chemicals: conversion of sugars to furan derivatives by catalytic processes, Appl. Catal. A: Gen. 385 (2010) 1–13.
[3] D. Sengupta, R.W. Pike, T.A. Hertwig, White paper on integrating biomass feedstocks into chemical production complexes using new and existing processes, 2008.
[4] A. Corma, S. Iborra, A. Velty, Chemical routes for the transformation of biomass into chemicals, Chem. Rev. 107 (2007) 2411–2502.
[5] J.-M. Lavoie, W. Baré, M. Bilodeau, Depolymerization of steam-treated lignin for the production of green chemicals, Bioresour. Technol. 102 (2011) 4917–4920.
[6] G.D. Yadav, R.V. Sharma, S.O. Katole, Selective dehydration of glycerol to acrolein: development of efficient and robust solid acid catalyst MUICaT-5, Ind. Eng. Chem. Res. 52 (2013) 10133–10144.
[7] G.D. Yadav, P.A. Chandan, D.P. Tekale, Hydrogenolysis of glycerol to 1,2-propanediol over nano-fibrous Ag-OMS-2 catalysts, Ind. Eng. Chem. Res. 51 (2012) 1549–1562.
[8] G.D. Yadav, P.A. Chandan, N. Gopalaswami, Green etherification of bioglycerol with 1-phenyl ethanol over supported heteropolyacid, Clean Technol. Environ. Policy 14 (2011) 85–95.
[9] M. Kleinert, T. Barth, Phenols from lignin, Chem. Eng. Technol. 31 (2008) 736–745.
[10] R. Bai, H. Zhang, F. Mei, S. Wang, T. Li, Y. Gu, G. Li, One-pot synthesis of glycidol from glycerol and dimethyl carbonate over a highly efficient and easily available solid catalyst NaAlO2, Green Chem. 15 (2013) 2929–2934.
[11] G.D. Yadav, P. Aduri, Aldol condensation of benzaldehyde with heptanal to jasminaldehyde over novel Mg–Al mixed oxide on hexagonal mesoporous silica, J. Mol. Catal. A: Chem. 355 (2012) 142–154.
[12] D.P. Debecker, E.M. Gaigneaux, G. Busca, Exploring, tuning, and exploiting the basicity of hydrotalcites for applications in heterogeneous catalysis, Chem. (Weinheim an der Bergstrasse, Germany) 15 (2009) 3920–3935.
[13] Kazuhiro Sugamoto, Yoh-ichi Matsushita, Takanao Matsui, Solvent free oxidative coupling of 2-naphthols catalyzed by hydrotalcite like compounds in aerobic conditions, Lett. Org. Chem. 9 (2012) 263–266.
[14] A.R. Massah, Mitra Toghyani, Batool Hojati Najafabadi, Green and efficient method for the acylation of amines and phenols in the presence of hydrotalcite in water, J. Chem. Res. 36 (2012) 603–605.
[15] A. Kumar, K. Iwatani, S. Nishimura, A. Takagaki, K. Ebitani, Promotion effect of coexistent hydromagnesite in a highly active solid base hydrotalcite catalyst for transesterifications of glycols into cyclic carbonates, Catal. Today 185 (2012) 241–246.
[16] M. Mokhtar, T.S. Saleh, S.N. Basahel, Mg–Al hydrotalcites as efficient catalysts for aza-michael addition reaction: a green protocol, J. Mol. Catal. A: Chem. 353–354 (2012) 122–131.
[17] G.D. Yadav, G.P. Fernandes, Selective synthesis of natural benzaldehyde by hydrolysis of cinnamaldehyde using novel hydrotalcite catalyst, Catal. Today 207 (2013) 162–169.
[18] S. Nishimura, A. Takagaki, K. Ebitani, Characterization, synthesis and catalysis of hydrotalcite-related materials for highly efficient materials transformations, Green Chem. 15 (2013) 2026–2042.
[19] F. Cavani, F. Trifir&#x00F2, A. Vaccari, Hydrotalcite-type anionic clays: preparation, properties and applications, Catal. Today 11 (1991) 173–301.
[20] T. Weschler, Taking Charge of Your Fertility, revised ed., HarperCollins, New York, 2002.
[21] A.M. Truscello, C. Gambarotti, M. Lauria, S. Auricchio, G. Leonardi, S.U. Shisodia, A. Citterio, One-pot synthesis of aryloxypropanediols from glycerol: towards valuable chemicals from renewable sources, Green Chem. 15 (2013) 625–628.
[22] D.M. Dishong, C.J. Diamond, M.I. Cinoman, G.W. Gokel, Crown cation complex effects. 20. Syntheses and cation binding properties of carbon-pivot lariat ethers, J. Am. Chem. Soc. 105 (1983) 586–593.
[23] W.P. Shum, H. Mazurek, J. Chen, Process for producing enantiomerically enriched guaifenesin, Google Patents, 1996.
[24] Z. Yao, S. Gong, T. Guan, Y. Li, X. Wu, H. Sun, Synthesis of ranolazine metabolites and their anti-myocardial ischemia activities, Chem. Pharm. Bull. 57 (2009) 1218–1222.
[25] Z.A. Bredikhina, V.G. Novikova, D.V. Zakharychev, A.A. Bredikhin, Solid state properties and effective resolution procedure for guaifenesin 3-(2-methoxyphenoxy)-1,2-propanediol, Tetrahedron: Asymmetry 17 (2006) 3015–3020.
[26] I.A. Sayyed, A. Sudalai, Asymmetric synthesis of L-DOPA and (R)-selegiline via, OsO4-catalyzed asymmetric dihydroxylation, Tetrahedron: Asymmetry 15 (2004) 3111–3116.
[27] M.J. Climent, A. Corma, S. Iborra, A. Velty, Activated hydrotalcites as catalysts for the synthesis of chalcones of pharmaceutical interest, J. Catal. 221 (2004) 474–482.
[28] P.T. Tanev, T.J. Pinnavaia, A neutral templating route to mesoporous molecular sieves, Science 267 (1995) 865–867.
[29] G.D. Yadav, J.Y. Salunke, Selectivity engineering of solid base catalyzed O-methylation of 2-naphthol with dimethyl carbonate to 2-methoxynaphthalene, Catal. Today 207 (2013) 180–190.

Please cite this article in press as: S.L. Bhanawase, G.D. Yadav, Activity and selectivity of different base catalysts in synthesis of guaifenesin from guaiacol and glycidol of biomass origin, Catal. Today (2016), http://dx.doi.org/10.1016/j.cattod.2016.12.008

[30] G.D. Yadav, J.J. Nair, Sulfated zirconia and its modified versions as promising catalysts for industrial processes, Microporous Mesoporous Mater. 33 (1999) 1–48.
[31] G.D. Yadav, T.S. Thorat, Kinetics of alkylation of p-cresol with isobutylene catalyzed by sulfated zirconia, Ind. Eng. Chem. Res. 35 (1996) 721–731.
[32] Y. Wang, W.Y. Huang, Y. Chun, J.R. Xia, J.H. Zhu, Dispersion of potassium nitrate and the resulting strong basicity on zirconia, Chem. Mater. 13 (2001) 670–677.
[33] S.L. Bhanawase, G.D. Yadav, Green synthesis of vanillyl mandelic acid (sodium salt) from guaiacol and sodium glyoxylate over novel silica encapsulated magnesium hydroxide, ACS Sustain. Chem. Eng. 4 (2016) 1974–1984.
[34] M.S. Tiwari, G.D. Yadav, Kinetics of Friedel–Crafts benzoylation of veratrole with benzoic anhydride using Cs2. 5H0. 5PW12O40/K-10 solid acid catalyst, Chem. Eng. J. 266 (2015) 64–73.

Please cite this article in press as: S.L. Bhanawase, G.D. Yadav, Activity and selectivity of different base catalysts in synthesis of guaifenesin from guaiacol and glycidol of biomass origin, Catal. Today (2016), http://dx.doi.org/10.1016/j.cattod.2016.12.008